Experimental Investigation of Initial Deployment of Inflatable Structures for Sealing of Rail Tunnels

Eduardo M. Sosa[1]*; Gregory J. Thompson[2]; Ever J. Barbero[3]

Abstract

Large-scale inflatable structures have become a viable alternative for sealing segments of large-diameter conduits or rail transit tunnel sections for preventing propagation of flooding, noxious gasses or smoke. In such applications, the inflatable structure is prepared for placement, either permanently or temporally, and maintained ready for deployment, inflation, and pressurization when needed. The sealing effectiveness depends on the ability of the inflatable structure to self-deploy and fit, without human intervention, to the intricacies of the perimeter of the conduit being sealed. This work presents results of experimental work performed for the evaluation of initial deployment and inflation of a prototype inflatable structure installed in a rail transit tunnel segment for containment of flooding. Folding and packing procedures necessary to prepare and install a full-scale inflatable in the tunnel segment are described. Methods for evaluation of conformity and degree of contact of the membrane with the tunnel section are implemented as well. Test results indicate that a successful distribution of the membrane material over the tunnel perimeter is achieved by a combination of gradual unrolling and controlled membrane release. The membrane distribution during the initial unfolding and inflation, the shape of transitions at corners and angles in the tunnel perimeter; the oversizing of membrane material in the hoop perimeter of the inflatable, as well as the surface texture of the membrane, were identified as main factors that affect the level of conformity and degree contact between the inflatable structure and the tunnel perimeter.

Keywords: Confined Inflatable; Conformity; Contact; Deployment; Folding; Membrane; Tunnel

---

[1]* Research Associate Professor, Department of Mechanical and Aerospace Engineering, West Virginia University, Morgantown, WV 26506-6106, USA. (Corresponding author) e-mail: eduardo.sosa@mail.wvu.edu

[2] Associate Professor, Department of Mechanical and Aerospace Engineering, West Virginia University, Morgantown, WV 26506-6106, USA, e-mail: gregory.thompson@mail.wvu.edu.

[3] Professor, Department of Mechanical and Aerospace Engineering, West Virginia University, Morgantown, WV 26506-6106, USA, e-mail: drb@wvu.edu.

Introduction

The protection of underground civil infrastructure is a high priority for transportation and security

agencies. In particular, rail transit tunnels running under bodies of water are susceptible to disruptions due

to flooding originated by extreme climatic events such as hurricanes, fires or other human-made events

(Federal Highway Administration, 2003; TCRP, 2006; Rabkin, 2007; Brezhnev et al., 2005). Some

examples of such incidents in the United States include the 1992 Chicago freight tunnel flood (Inouye and

Jacobazzi, 1992) which forced the shutdown of the subway system, caused damage to numerous

businesses and required the evacuation of about 250,000 people from the area. In 2003, Hurricane Isabel

caused flooding of the Midtown Tunnel in Virginia. During this event, about 167,000 m^3 of water from

the Elizabeth River flooded the tunnel system in just 40 minutes. The flooding left the tunnel damaged

and closed for nearly a month (Post et al., 2005). Most recently, in New York City, seven subway tunnels

under the East River as well as three road tunnels flooded during Hurricane Sandy and remained

inoperable for several days (NYC Office of the Mayor, 2013 and Zimmerman, 2014). These incidents and

others summarized in Leitner (2001), Kirkland (2002), Haack (2002) and TCRP (2006) have demonstrated

a need for research on ways to mitigate vulnerabilities or, at least, minimize the consequences of

catastrophic events. Although it is impossible to prevent all situations that can lead to flooding, damage

can be substantially minimized by reducing the area affected by the event. To minimize the effects of any

eventual threat, a possible approach is to compartmentalize the tunnel system (Tan, 2002). However, it

can be difficult, if not impossible, to install or repair in an existing tunnel all the elements required for

compartmentalization. Typically, space constraints inhibit the installation of new protective devices such

as flood gates. The elevated cost of interrupting the tunnel operations or making major infrastructure

modifications have also discouraged attempts to improve the tunnel resilience by these means.

In the recent years, alternative solutions have been proposed to seal tunnel segments susceptible to the consequences of extreme events. In particular, large inflatable structures for protection of civil transportation infrastructures, such as railway tunnels, large pipes or mines, have been under development in the recent years as reported by Barrie (2008), Martinez et al. (2012), Fountain (2012), Lindstrand (2013) and Stocking (2013). Large scale inflatable dams for flooding control have also been studied by Carter et al. (2001), Ghavanloo and Daneshmand (2010) and Sklerov and Padilla (2012).

The implementation of large-scale inflatable structures (also called inflatable plugs) inside transportation tunnels intends to prevent or reduce the damage induced by hazardous events by creating a compartment to contain the threat (Tan, 2002). Potential threats include flooding, smoke or noxious gasses that can propagate through a tunnel system and compromise its functionality and structural integrity. The idea is that one or more inflatable structures are installed at specific locations of the tunnel to create a compartment that can isolate the compromised region (Tan, 2002; Martinez et al., 2012). Recently, Barbero et al. (2013a, b) and Sosa et al. (2014a-c) reported testing efforts to demonstrate the feasibility of containing flooding with large inflatable structures. Under these efforts, multiple tests were performed at different scales using specially built testing facilities designed to simulate flooding of a tunnel segment.

The implementation of inflatable structures for sealing of rail transit tunnel segments can be divided into three main phases: I-Preparation and installation of the inflatable; II-Deployment; and III-Pressurization.

Phase I requires the definition and implementation of a folding sequence in conjunction with the packing of the folded plug in a storage container. This phase also includes the transportation and installation of the folded plug at specific locations inside the tunnel segment to be sealed, leaving it ready to be activated when needed.

Phase II begins with automatic opening of the storage container, which allows the liberation of the inflatable followed by inflation until it reaches its final shape and position within the tunnel section. The deployment and initial inflation of the plug are performed using air at relatively high flow rates, typically in the range of 25 to 50 m^3/min, to allow rapid expansion and positioning of the inflatable which can be achieved in the range of 2 to 5 minutes. With these air flow rate levels, the internal pressure of the plug is relatively low, in the range of 2 to 7 kPag (Barbero et al., 2013b; Sosa et al., 2014a).

Phase III begins immediately after the initial positioning achieved by high-flow and low-pressure inflation implemented in Phase II is complete. In Phase III, the plug is pressurized so it can withstand, predominantly by friction, the external pressure originated by flooding. The magnitude of the pressurization depends on the level of flooding pressure expected to be contained. For example, in the full-scale tests performed by Barbero et al. (2013b) and Sosa et al. (2014a), the inflatable plug was pressurized up to 117 kPag and then subject to water flooding at a pressure of 80 kPa. These tests demonstrated that the sealing capacity of the pressurized inflatable is highly influenced by the level of local and global conformity achieved during Phase II, which in turn depends on how the inflatable was prepared in Phase I (Barbero et al., 2013b; Sosa et al., 2014a).

With the previous considerations, the work presented here is completely focused on the analysis and understanding the results of experimental evaluations corresponding to Phases I and II delineated previously. Folding and packing procedures that can be implemented in a full-scale inflatable along with the need for implementation of passive mechanisms for controlled release of the membrane are described in detail. Experimental results of initial deployment and inflation tests are presented and discussed for the purpose of identifying key aspects of the deployment dynamics that influence the sealing capacity of the inflatable plug once it is fully positioned in the tunnel. Methods developed for evaluating conformity, and

the results of their implementation in the experimental evaluations are described in detail as well.

The outline of this paper is as follows: an overview of the characteristics of the full-scale prototype inflatable plug used for the tests are presented first. Folding and packing procedures are described next, followed by an overview of the full-scale test setup and the two methods developed for evaluation of conformity. Test results and discussions followed by a summary of significant observations, considerations for implementation and conclusions are presented at the end.

Inflatable Plug

The full-scale prototype inflatable plug manufactured for the test presented here consists of a cylindrical segment closed by two hemispherical end caps. The cylindrical segment has a diameter of D_c = 4.940 m and a length L_c = 4.641 m. The radius of each hemispherical end cap is R = 2.469 m, and the total length of the plug is L_T = 9.581 m (Figure 1-a). The design, including the shape and dimensions, is based on the procedures proposed by Barbero et al., 2013a and Sosa et al., 2014c. The design is based on the premise that the stability of the plug is achieved by providing sufficient frictional force to counteract an external force such as a flooding pressure. The frictional forces are generated by the contact between the membrane of the cylindrical segment of the inflatable and the surrounding inner perimeter of the tunnel section where the plug is deployed and pressurized. The length of the cylindrical segment is determined based on friction tests run at the coupon level on samples of membrane materials and validated by reduced-scale prototypes subjected to induced slippage under wet conditions (Sosa et al., 2014b). The same prototype was used for full-scale flooding simulations to demonstrate the ability of the inflatable to remain in equilibrium while containing the flooding pressure with manageable leakage rates as described in Barbero et al., 2013b and Sosa et al., 2014a.

The perimeter of the cylindrical portion was designed to cover elements that typically exist in a tunnel segment, such as duct banks, pipes, cables, and rails. Typically, the design of the perimeter of the cylindrical portion of the plug accounts for all the elements present in the tunnel that should be covered by the membrane. In an ideal design, the oversizing of the membrane would be no more than 1% to 2% of the nominal perimeter to cover, and this percentage of oversizing is accounted as part of the manufacturing tolerance. However, preliminary tests performed using a surrogate inflatable plug demonstrated that the deployment and distribution of the membrane are not uniform. These preliminary results demonstrated a tendency of portions of the membrane to create local bridging close to corners, transitions or around pipes when only the manufacturing tolerance was added as oversizing. This situation led to investigate further on how much oversizing would be necessary to reduce the formation of bridging around the contact perimeter. Additional tests were performed using a surrogate inflatable with a 10% oversizing. Test results with this level of oversizing demonstrated that although the formation of localized bridging was practically eliminated, the formation of large longitudinal wrinkles increased, demonstrating that there was an excess of membrane material in the contact perimeter. Smoke tests that followed the deployment and inflation demonstrated that those longitudinal wrinkles are prone to become leakage passages that may reduce the sealing capacity of the inflatable plug. A second iteration reducing the oversizing to 5% was performed next. With this percentage of oversizing, all the elements present in the tunnel perimeter were covered without visible bridging and with fewer wrinkles which were mostly concentrated on the lower portion of the tunnel perimeter. Smoke tests performed with this level of oversizing also showed a better sealing capacity. Based on this preliminary evaluations, the final testing unit was manufactured with an oversizing of 5% that was added to the nominal circumferential perimeter of the cylindrical portion of the inflatable plug. This percentage ensured contact of the plug membrane

with the tunnel perimeter with minimum formation of large wrinkles or bridging that could reduce the sealing capacity of the plug. Overall, in the design of the portion of the plug that will be in contact with the tunnel perimeter, the length of the cylindrical portion of the plug provides the necessary contact length for the development of frictional forces to maintain the axial stability, while the circumferential perimeter of the cylinder ensures local conformity of the plug to the tunnel cross-sectional perimeter to minimize leakage, and therefore maximizing the sealing capacity of the plug.

Regarding the construction of the membrane of the inflatable plug, it consisted of a three-layer system comprised of an internal bladder, an intermediate protective fabric, and an external macro-fabric as shown in Figure 1-b. The bladder is the innermost layer of the construction and is in direct contact with the fluid used for inflation and pressurization. The function of the intermediate fabric is to protect the inner bladder from protruding through the external macro-fabric. This intermediate protective fabric can be made of different high-strength fibers such as Vectran or Kevlar. The outermost layer is a macro-fabric comprised of woven webbings in a plain weave pattern. The webbings of the macro-fabric are 5 cm wide, 3 mm thick and are manufactured with Vectran fibers (Kuraray, 2013). Structurally, the outermost layer is the most important since it carries the membrane stresses and shear stresses (Peil et al., 2012) generated by the pressurization while the two inner layers provide watertightness and contribute to the total mass and volume of the membrane. The two innermost layers were oversized 2% during the manufacturing process with respect to the outer layer to ensure that not membrane stresses were carried during the pressurization process. Two metallic fittings for inflation and air-release were also integrated into the membrane of one of the hemispherical end caps. The total mass of the inflatable plug including inflation fittings was approximately 907 kg.

It is important to emphasize that while the concept of deploying an inflatable plug can potentially be

applied to any shape and size of tunnel, design parameters such as contact length, percentage of oversizing of the circumferential perimeter, as well as the multi-layer membrane configuration to assure the necessary strength to withstand the inflation and flooding pressures, are all tied to the particular conditions of the tunnel under consideration. The design of inflatable tested under this research effort is anticipated to work in tunnels with mostly circular cross sections, with equivalent diameters in the range of 4 to 6 meters. Tunnels with other cross-sectional shapes, with similar equivalent diameters, could benefit from the design tested in this research as well. For those tunnel shapes, the equivalent diameter, which is defined as $D_e = p_e / \pi$, and where p_e is the estimated contact perimeter for a given shape (rectangular, square, horseshoe or other polygonal shapes), can be used to determine the size of the equivalent cylinder that will be in contact with all the walls of the tunnel shape under consideration. The length of the equivalent cylinder, as well as the strength of the membrane, will be a function of the external pressure to withstand and the level of pressurization, respectively, necessary to maintain the stability of the inflatable.

Folding and Packing

The definition of the folding and packing sequences required multiple iterations to determine an effective method to systematize the process so that it produced repeatable results during the deployment tests. The dimensions and weight of the inflatable plug were the two main factors that drove the development and implementation of a repeatable folding and packing sequence that could be implemented manually by a set of skilled operators in a consistent fashion. The folding sequence that proved to be most effective is summarized graphically in Figure 2 and consisted of the following steps:

Step 1: The sequence began with an unconstrained inflation at low pressure (less than 1 kPag). Reference lines marked on the plug and on the floor were aligned as illustrated in Figure 2-a. The initial

unconstrained inflation also served for doing a visual inspection of the integrity of the surface along with re-aligning and untwisting of webbings on the surface of the plug.

Step 2: A controlled deflation began maintaining the alignment of the reference lines R1 and R2. The parallelism of the reference lines was maintained by gradually rolling of the plug to correct deviations until the two lines converged at the floor. Simultaneous to the deflation, the center portions of the hemispherical end caps were moved inward as part of the beginning of the folding process, as illustrated in Figure 2-b.

Step 3: Once the deflated plug was lying on the floor, it created a flat surface with a shape close to a projection of the cylindrical and hemispherical portions of the plug on the floor. Remaining wrinkles were eliminated by a manual gentle stretch of the membrane until most wrinkles were removed, and the membrane was nearly flat. One of the longitudinal edges of the cylindrical segment was partially folded along the cylindrical portion of the plug to allow positioning and alignment of the portable storage container as shown in Figure 2-c. The attachment of the deflated plug to the base of the container started matching reference line R1 marked in the plug with a reference line marked in the interior of the container. The plug was connected to the container by weaving a strap between the longitudinal webbings of the plug and C-shaped metal webbing guides preinstalled at the base of the container. The longitudinal strap was later tensioned to ensure that the inflatable plug will remain in position and attached to the container during the initial deployment and subsequent testing operations.

Step 4: After finishing the attachment of the plug to the base of the container, the folding sequence of the cylindrical portion of the plug began. Line L1, located 6 m from the edge of the container, was joined to line L2 located 2.4 m from line L1 as shown in Figure 2-d. The position and separation of lines L1 and L2 was determined based on the position of features placed on the ceiling of the tunnel perimeter where

more membrane material would be needed to maximize the coverage. Once lines L1 and L2 were coincident, they were connected at discrete points spaced every 45 cm as illustrated in Figure 2-e. The connectors consisted of nylon tie-downs with a nominal individual capacity of 0.8 kN. The purpose of creating this initial fold and connection at discrete points is to create a temporary crease that later, during the initial inflation, and upon breakage of the tie-downs, will release the membrane material "stored" between lines L1 and L2. The liberated membrane material will then contribute to improving the coverage of ancillary items typically installed in the ceiling and laterals of the tunnel section. The installation of the tie-downs provided a passive mechanism that allowed controlled release of the membrane.

Step 5: The folding sequence continued by successive flat rolling the membrane material. In Figure 2-f, reference line L3 was joined to lines L1/L2. Two additional flat rolls were necessary for reaching line L4 located at the bottom portion of the membrane. Before completing the folding of the cylindrical portion of the plug, additional handling was necessary to flatten the hemispherical end caps and to eliminate residual wrinkles generated by the previous folds. At this point, the folded plug is ready to be placed inside the container as illustrated in Figure 2-g.

Step 6: Reference line L4 shown in Figure 2-g was placed inside the container by a combination of rotations around the longitudinal axis of the container. Once the folded plug was completely inside the container, further handling was necessary for final flattening the different portions of the plug, and for eliminating wrinkles generated by the previous folds. The inflation port was tethered to the interior of the container to limit unnecessary rotations and translations during the initial unrolling as illustrated in Figure 2-g.

Step 7: With the plug inside the portable container, the soft-cover of the container was closed. The two halves of the soft-cover were tensioned by tightening of the cinch laces located in one of the halves.

The tightening of the soft-cover produced a stiff surface that held the folded plug in place within the container without bulging as illustrated in Figure 2-h. Final maneuvers included the transportation of the container and its installation within the tunnel section (Figure 2-i). Steps 1 to 7 were repeated for every deployment and inflation test.

Test Setup

The full-scale testing facility consists of a mock-up tunnel segment specially built to replicate a segment of a typical rail transit tunnel. The tunnel segment is 15 m long and 4.75 m inner diameter. The interior of the tunnel mockup was refitted to reposition and cover cables, pipes and other features that can be found in typical rail transit tunnel. The refitting included raising the floor in a form similar to a grade crossing where the rails do not protrude from the surface. The contact perimeter included smoothed corners as wells as rounded or chamfered transitions created to minimize bridging of the membrane. All these modifications were introduced to maximize the sealing capacity of the plug. The refitting of the tunnel interior was made in consultation with tunnel owners and operators who provided guidance on what elements can be repositioned, covered, or removed within the operational limits of existing tunnels. Figure 3-a shows the resulting tunnel cross-section after the refitting. Figure 3-b shows lateral and rear views of the tunnel mockup used for testing.

The inflation system was designed and built to operate with air during the initial inflation and then with water during full pressurization of the inflatable. Considering that this work is focused only on the initial deployment and inflation, only the main components relevant to this operation are outlined here. The initial deployment and inflation of the plug required a low-pressure, high-flow centrifugal fan connected to the inflation port of the plug by a set of rigid and flexible hoses as illustrated in Figure 4-a.

The air flow rate was measured with a 20-cm diameter laminar flow element (LFE) installed in the pipeline. The air fan was also connected to an automatic control system that regulated the air flow rate and monitored inflation pressure in the plug. Figure 4-a shows an overview of the actual components of the air inflation system. Figure 4-b illustrates a schematic of the test setup. Figure 4-c shows the final position of the container with the folded plug in its interior right before the beginning of a deployment and inflation test. As indicated earlier, multiple preliminary tests were necessary to adjust the deployment and inflation process. Once an optimal testing configuration was established, a total of six additional tests were executed using this test configuration to verify the repeatability and consistency in the results. The results and observations made during this last set of six tests are described in the next sections.

Methods for Evaluation of Conformity

The evaluation of conformity was carried out by using two methods designed to quantify the level of local conformity of the inflated plug to the tunnel perimeter. The first method (M1) is based on inspection of specific locations on the perimeter of the plug accessible from the open end of the tunnel mockup. Under this evaluation method, numerical grades are assigned to specific zones considered critical for the success of a test. Nine locations in the tunnel perimeter were identified as critical zones based on its potential for becoming sources of significant leakage due to poor local conformity or complete lack of contact with the membrane. These locations typically included corners, changes of direction in the perimeter or presence of protrusions. Each location was qualified by a weighted grade based on the level of conformity of the membrane to the tunnel perimeter observed during the inspections. In general terms, good levels of local conformity would lead to a higher global grade, and lower levels of conformity or no contact in one or several locations would lead to a lower global grade. The maximum score that a

12

deployment test could get is ten (excellent global alignment, good local contact, no local gaps), and the minimum is zero (severe misalignment, multiple gaps, no contact). A limitation of method M1 is that the evaluations are based on the inspection of the visible side of the plug. Method M1 assumes that the level of local conformity seen in the visible end of the plug remains constant along the entire contact length of the plug, which may not be necessarily accurate for all the tests that were evaluated under this method. Despite this limitation, the implementation of method M1 served as a tool to quantify the quality of each deployment, which led to a better understanding of the deployment process.

The second method (M2) implemented to evaluate local contact at critical locations is based on the information provided by electrical contact sensors located along select longitudinal lines in the tunnel perimeter where preliminary testing showed poor local conformity. The sensors detected contact between the membrane and the tunnel surface developed along the cylindrical portion of the plug. Seven metallic strips, with eight contact sensors each, were installed at locations considered critical for successful sealing. The installation of multiple sensing strips allowed the simultaneous detection of contact at corners, transitions and other singularities along the cylindrical portion of the plug and around the tunnel perimeter. The information collected by the sensors was combined in a contact map that allowed direct monitoring of the evolution of contact as the test progressed. Under method M2, the quality of local conformity was measured by the number of sensors activated during the test with respect to the total number of sensors available at each one of the sensing lines and expressed as percentages at local and global levels. The implementation of method M2 was not intended to verify watertightness at the local or global level. The main purpose of implementing method M2 was to detect the existence of contact, regardless of the magnitude, along with critical positions in the tunnel perimeter where the implementation of evaluation method M1 was not longer practicable.

Test Results and Discussion

Deployment and Inflation

The deployment of the plug started with the automatic activation of the opening mechanism installed in the vertical soft-cover of the container. The opening mechanism released the pre-tension of the soft-cover liberating the folded plug, which started to unroll by its weight and gradually moved out of the container as the air inflation began. The air inflation process consisted of two stages: 1) Initial inflation at a constant air flow rate of 42 m^3/min until the plug was fully inflated and positioned in the tunnel; 2) Once the plug was fully inflated, the air flow rate was reduced to 1.4 m^3/min, and the internal pressure was kept constant at 2 kPag. With this test configuration, the total time from initial deployment to full inflation ranged from 2.7 to 3.1 minutes with an average of 2.9 minutes as summarized in Table 1. In all the initial inflations, the internal pressure was kept constant at 2 kPag. The limit of 2 kPag was the minimum pressure to maintain the shape of the inflatable in place after completion of the initial inflation. This value is a function of the weight of the membrane that needs to be kept in contact with the inner tunnel perimeter. This level of pressure also allowed the researchers to safely approach to the inflatable for evaluation of local conformity without the risk of sudden depressurization. Previous studies have shown that an overpressure in the range of 20 kPag to 35 kPag can produce minor, moderate, and major eardrum ruptures. Also, overpressures higher than 35 kPag will rupture eardrums in about 1% of subjects exposed to the overpressure (Richmond et al., 1989; Fraser, 1989; Beveridge, 1998; Stewart, 2006-a-b). The pressure of 2 kPag was well below those thresholds and allowed safe implementation of evaluation method M1.

Figure 5 shows an example of the sequence of initial deployment and air inflation corresponding to Test #4 where the inflation progresses from, first, unfolding from the lateral container and falling onto the

tunnel floor, and then, by successive unrolling as the air inflow pushes the membrane against the opposite vertical wall. When the inflatable cannot move further laterally, the inflation continues upwards until reaching the tunnel ceiling. All tests displayed a similar pattern of membrane unrolling and distribution as it reached the final position in the tunnel. The final position of the inflatable at the end of the inflation process of each test is illustrated in Figure 10.

Figure 6-a shows an example of air flow rate and inflation pressure recorded for Test #5. The air flow rate was kept constant until the pressure exceeded 0.5 kPag, at which point the control system automatically started reducing the air flow rate as the pressure reached the target value of 2 kPag. The variation of internal pressures for the different tests as the inflation progressed are illustrated in Figure 6-b. These results show that the inflation pressure remained approximately constant around 0.10 kPag for approximately the first two minutes of the inflation. During these two minutes, the air flow gradually filled about two-thirds of the volume of the plug as illustrated in the sequence of Figure 5. Then, during the last minute, the inflation pressure reached its first peak which triggered the intended breakage of the tie-downs installed during the folding procedure. The progressive breakage of tie-downs produced a gradual release of membrane material, which also increased the volume of the plug producing a temporary decrease in the inflation pressure. Since the centrifugal fan continued providing a constant air flow rate, the pressure rose again until all the tie-downs broke, and the membrane was completely free to expand and reach the ceiling of the tunnel. Ideally, a single peak in the inflation pressure history would indicate a simultaneous breakage of all tie-downs. However, tests results showed two or three consecutive peaks suggesting that the breakage of the tie-downs was gradual and originated the fluctuations in the inflation pressure seen in the last minute of the inflation as illustrated in Figure 6-b. For all the tests, these successive fluctuations during the third minute of the inflation time ranged between 0.3 to 0.7 kPag before reaching the constant target

value of 2 kPag.

An estimation of the force acting on the tie-downs at the onset of intended failure is summarized in Table 2. In this table, R is the estimated equivalent radius of the plug at the instant of failure of the tie-downs. From the videos and pictures taken during the deployments, it was estimated that the radius R of the plug at the onset of failure of the tie-downs was between 2.2 to 2.3 meters. The pressure P_i was estimated from the peaks observed during the third minute of the total inflation time. The hoop stress in the cylinder for an unconstrained inflation is the product of R and P_i (expressed in terms of force per unit of length). The total force is the product of the hoop stress and the nominal length of the cylindrical portion of the plug ($L_c = 4.641$ m). The force per tie-down is the ratio between the total hoop force and the number of tie-downs installed during the folding procedures (ten units). Then, the axial force taken by an individual tie-down is around 0.75 kN, which is close to the nominal capacity of each tie-down (0.8 kN).

The effects of having an inflation with a controlled membrane release are illustrated in Figure 7. In Figure 7-a, experimental results corresponding to Test #5 are compared to a finite element simulation of the initial deployment and inflation of the plug. A sequence of transversal cross-sections of the inflatable was obtained by post-processing the finite element simulation in order to illustrate how tie-downs temporarily held the membrane during the inflation. The sequence of simulation results of Figure 7-b shows how the inflation progresses until the membrane stored between tie-downs is released and pushed up by the inflation pressure to the ceiling of the tunnel. The transversal cross-sections illustrated in Figure 7-b also illustrate the level of conformity of the membrane to the perimeter of the tunnel cross-section at the end of the inflation. Further details on how the finite element models were generated and further simulation results can be found in Sosa et al., 2016.

The level of local conformity is particularly important to maximize the sealing capacity of the plug.

Experimental tests demonstrated that even when the plug is pressurized to the required internal pressure to withstand the flooding pressure, the very low extensibility of the membrane in combination with the friction between the membrane and the tunnel surface, locked the plug in place. Under these conditions, any local gaps and local bridging created by wrinkles or misalignments of the membrane remained open (Barbero et al., 2012b; Sosa et al., 2014a). The need of maximizing the sealing capacity of the plug led to the systematic implementation of tie-downs as a passive control mechanism to drive and control the release of the membrane material. This technique contributed to improving the coverage of the plug membrane over critical regions of the tunnel perimeter including corners, changes of curvature and sharp angles located around tunnel contact perimeter.

Evaluation of Conformity

The conformity of the plug to the tunnel section was evaluated at the end of the air inflation. Evaluation method M1 described previously was implemented for all the tests. Preliminary trials showed that a minimum score of 7 out of 10 was necessary to proceed with the flooding simulations. For the tests reported in this work, scores ranged from 7.5 to 9.3, with an average of 8.4 as summarized in Table 1. These results are indicative of a relatively good level of conformity of the plug to the tunnel section as seen from the open end of the tunnel. Figure 8-a shows an example of the evaluation and evaluation form completed for Test #6. Tests #3 and #6 were the tests in which the best level of local conformity was observed as reflected in their scores of 9.1 and 9.3, respectively, as summarized in Table 1. Figure 8-b shows close-up views of critical locations illustrating the good degree of contact between the membrane and the tunnel contour.

Method M2 was implemented to evaluate contact along the cylindrical portion of the plug where the

visual inspection was not possible. Figure 9-a shows the position of strips with contact sensors around the tunnel perimeter. Figure 9-b shows the position of the contact sensors in the region of the tunnel where the cylindrical portion of the inflatable would sit. The information collected from the sensors was compiled in contact maps like the one illustrated in Figure 9-c. The contact maps were created following a conical perspective where each concentric ring of the contact map corresponds to a position R_i in the tunnel along the contact length of the plug where the contact sensors were placed following the sequence illustrated in Figure 9-b. Table 1 shows that for the global results obtained with the contact sensors used in evaluation method M2. Values summarized in Table 1 indicated that global values for M2 ranged from a minimum of 60% obtained in Test #1, to a maximum of 94% obtained in Test #3. The global average for method M2 was 78%.

A break-down of the local contact detected by the contact sensor at each position P_i for all the tests is summarized in Table 3. Results show that values at each position ranged from 50% to 94%, with an average of 78%. Having at least 6 sensors out of a total of 8 (~75%) showing contact at the different positions (P1 to P7) was indicative of a relatively good degree of local conformity and suggested "strong" contact along the lines that were not accessible for visual inspection. On the contrary, when just a few sensors (less than 5 or ~62%) were detecting contact at a particular sensing line, the quality of contact at the line was considered "weak." The spatial distribution of contact along the cylindrical portion of the inflatable plug is illustrated in the contact maps of Figure 10 for Tests #1 to #6. The data for generating the contact maps illustrated in Figure 10 was captured at the end of the air inflation while the pressure was constant at 2 kPag.

Contact maps show that at position P1, as expected, the membrane of the cylindrical portion of the plug was practically in full contact with the ceiling of the tunnel during all six tests. Position P3, which is

located at the base of the container and where the plug is attached, is one of the most critical positions for achieving good levels of local conformity. Contact maps of Figure 10 show that in Test #1 there was no contact along line P3. For this particular test, the lack of local contact was originated by bridging of the membrane over the circular transition located at the base of the container. For the remaining tests, the circular transition was replaced by a flat transition and the single attaching line was split into attaching three lines separated 15 cm from each other to reduce the formation of membrane bridging. The effect of this modification is reflected in tests #2 to #6 for which practically full contact was achieved during every test.

The second critical location in terms of local conformity is at position P5. In three tests (#1, #3 and #6), a relatively strong contact (75%) was detected along line P5. These are considered good results since small local surface imperfections or wrinkles in the membrane can be attributed as possible reasons for the lack of local contact. Tests #2 and #4 show a relatively weak contact as only two out of eight and four out of eight sensors, respectively, detected contact along line P5. For the same position, the worst result was observed in Test #5 in which no contact was detected. Inspections performed during this test at this particular location indicated the existence of membrane bridging across the circular transition and along line P5 that created a gap between the membrane and the surface of the tunnel.

The third critical location in terms of local conformity is at position P6. At this position, weak contact was observed in Tests #1 and #4 (three out of eight sensors detecting contact, for both tests), as well as in Test #6 (four out of eight sensors). Relatively strong contact was achieved in Tests #2, #3 and #5 for which contact was detected by five out of eight sensors, seven out of eight sensors and all sensors, respectively.

A comparison of contact at positions P5 and P6 indicates that a better level of local conformity was achieved at position P6, with a local percentage of 63% (average of five out of eight sensors detecting

contact). While at position P5, a local percentage of only 50% (average of four of eight sensors detecting contact) was achieved at the end of the inflations. These two local percentages were the lowest of all values obtained from all the tests as summarized in Table 3. The apparently weak contact achieved along lines P5 and P6 is attributed to two reasons: a) partial bridging of the membrane over rounded transitions, which prevented contact of the membrane with some or all the sensors; b) the possible combination of the texture of the external layer of the plug membrane (see Figure 1), with the possible formation of local wrinkles along lines P5 and P6, along with the size (6-mm diameter) of the contact knob that was part of the sensor (see Figure 9-a), may have converged for not receiving a contact signal from the sensors that would appear in the contact maps of Figure 10. The worst case corresponded to Test #5 in which the membrane bridged all along line P5 creating a path for leakage observed during the flooding simulations. Despite the lack of contact in this particular corner, the inflatable plug remained stable and held the flooding pressure with a manageable global leakage rate as reported in Sosa et al. 2014a.

From the results obtained during the inspections, as well as from the contact maps illustrated in Figure 10, it is seen that the following factors influence the local conformity of the membrane along critical positions in the perimeter of the tunnel:

1) The first factor is related to how the membrane is distributed during the initial deployment and up to the end of the inflation. The initial distribution of the membrane is directly related to how the plug was folded during the preparation procedures. During the design and the development of an efficient method to fold and facilitate the deployment of the inflatable plug, it was found that in aerospace applications, inflatables are typically folded following two main patterns. One of the simplest folding patterns is the "z-fold" in which the inflatable is flattened before being simply folded back and forth at regularly spaced intervals at discrete lines or hinges. However, despite the simplicity, the discrete

nature of the folding creates a discontinuous structure that, during the inflation, restricts the air flow between sections and results in a structure that are sensitive to small changes in shape with an unpredictable and dynamically unstable deployment path (Schenk et al., 2014; Katsumata et al., 2014). In this work, attempts of implementing a z-fold for lateral deployment resulted in the entanglement of the membrane and poor local conformity. The second common folding pattern in aerospace applications is by rolling or coiling the deflated structure. This way of folding demonstrated to be an effective and compact method for folding and packing an inflatable structure with minimal residual creases (Schenk et al., 2014; Katsumata et al., 2014). Depending on the configuration, rolling can be in a single or multiple directions. For this folding method, it is also common to implement passive controls or retardation devices, such as coil springs, Velcro strips or tie-downs installed to produce a more predictable deployment by controlling the final unrolling velocity and minimizing the sudden release of sections. This technique results in a more controlled deployment that tends to be much more stable dynamically (Schenk et al., 2014). This second technique was implemented in this work. For a lateral deployment, this technique combined with the action of gravity produced a relatively smooth gradual unrolling of the inflatable from the container side to the opposite side as illustrated in the sequences of Figure 5 and Figure 7. This technique resulted in more uniform coverage of membrane over the lower portions of the tunnel perimeter especially at the intersection of the tunnel floor and the lateral duct banks.

2) A second factor, and related to the previous one, is the sequential release of membrane material held on the upper portion of the cylindrical segment of the plug and later released for covering the upper portion of the tunnel perimeter. The sequential release was achieved by gradual breakage of the tie-downs installed as passive restrainers during the folding process that released membrane material

during the last minute of the inflation process (see Figure 6-b and Figure 7-b). The gradual release of membrane material assured uniform coverage of the upper portion of the tunnel perimeter. For the experiments reported in this work, only one crease was created during the folding process. However, multiple smaller creases created at specific locations around the perimeter of the cylindrical portion of the plug could improve the level of conformity in more complicated tunnel profiles. Preliminary deployment tests including two creases, one to release material to cover the upper region of the tunnel and one to better seal the lower right corner of the tunnel (P5 in Figures 9 and 10), have shown similar behaviors and improved levels of local conformity. However, further tests will be necessary to evaluate the consistency and effectiveness of implementing multiple creases in other more intricate tunnel profiles.

3) The third factor is related to the shape of the transitions at corners and angles. Test results showed that the membrane could self-accommodate well to rounded transitions when the initial deployment and inflation are nearly flawless; however, repeated testing demonstrated the variability in the degree of local conformity and the tendency of the membrane to bridge rounded transitions at specific locations. The formation of local bridging was reduced in the container by the implementation of a flat transition between the curved vertical wall and the inner floor of the container. This modification contributed to minimizing the creation of gaps that can lead to increased leakage during flooding simulations. Similar modifications can be implemented around the contact perimeter at locations of changes of direction or ninety-degree corners. Considering the relatively low levels of local contact detected by the contact sensors, the lower right and lower left corners of the tunnel (P5 and P6 in Figure 9) would be the zones where flattening transitions or reducing the curvature will improve the local conformity.

4) The fourth factor is related to the oversizing of the hoop perimeter of the cylindrical portion of the

inflatable in comparison to the nominal tunnel perimeter. For this factor, preliminary evaluations along with the results reported in this work indicated that an oversizing of at least 5% is necessary to achieve acceptable levels of local conformity. Higher percentages could be beneficial for reducing the formation of gaps during the initial deployment if the material is properly released and distributed around the perimeter. But percentages of oversizing above 5% can also be counterproductive as large longitudinal wrinkles tend to form and lead to the formation of distortions in the contact surface with the subsequent increase in leakage rates.

5) The fifth factor that influences the local contact is the texture of the macro-fabric that constitutes the external layer of the inflatable. In the contact maps illustrated in Figure 10, there are several instances in which just one or two contact sensors are not detecting contact. In these instances, the lack of contact is attributed to the presence of localized small gaps in between the webbings or small wrinkles that prevent the contact. This factor can also be related to the roughness of the surface texture of the tunnel. This factor may not seem very critical, but the sum of small imperfections or localized roughness that contribute to the formation of gaps reducing the contact surface, adds to the volume of leakage that the inflatable intends to contain.

Considerations for Implementation

In addition to the considering the factors that influence the global and local conformity of the plug at the end of the initial deployment and inflation, the implementation of large-scale inflatable plugs for sealing segments of tunnels will require additional considerations to assure the integrity of the tunnel during the installation and operation of the inflatable. In this regard, the tunnel segment selected for housing the inflatable during the different stages of implementation will require:

1) <u>Availability of storage space</u>: As seen in the experimental work presented in the previous sections, the inflatable incorporates a compact folding that allows storage of all the membrane material and auxiliary components within a container that seat within the tunnel profile and without interfering with the dynamic envelope of the train. Storage areas can be located on top of lateral duct banks (as illustrated in Figure 4-c) or on the ceiling of the tunnel as described in Martinez et al., 2012.   The removable storage container is designed to minimize the total storage volume and maximize portability so the mounting and dismounting operations can be executed expeditiously. Additional space at nearby or remote locations will be necessary for storing pressurization and control equipment.

2) <u>Tunnel liner strength for initial pressurization</u>: Experimental results presented in the previous sections showed that the initial deployment and inflation can be achieved with a high-flow centrifugal fan that can provide volumetric flow rates of at least 42 m^3/min (~0.7 m^3/sec). This air flow rate can fill the total volume of the inflatable in about three minutes at a pressure of 2 kPag. Experimental results described in previous sections demonstrated that this level of pressure is sufficient to hold the inflatable in place while the pressurization system is activated. The relatively low level of pressure needed for the initial deployment and positioning of the inflatable will not generate significant stresses in the main liner of the tunnel segment that contains the inflatable. As a reference, pressure waves at nearly the speed of sound propagate in the interior of the tunnel when a train passes. Measurements for passing trains at speeds of nearly 200 km/h (55.5 m/sec) showed that the internal dynamic pressure originated by the pressure wave can reach peaks of 1.7 kPa (Rodler and Hagenah, 2012; Ricco et al., 2007). This level of pressure is in the same range and order of magnitude of the pressure exerted by the inflatable plug during the initial deployment and inflation sequence described in this work. The installation of an array of rugged contact sensors at key locations or checkpoints around the tunnel perimeter can be useful to monitor two aspects

of the deployment: first, that the inflatable has reached its intended position during the initial unrolling and inflation; second, the level of contact pressure reached at those checkpoints during the different stages of pressurization. The same array of sensors can provide the magnitude of contact pressure being transferred from the inflatable to the liner during the subsequent full pressurization.

3) <u>Tunnel liner strength for final pressurization</u>: Once the inflatable is fully deployed and positioned, the pressurization begins. The pressurization of the inflatable is necessary to assure that the frictional forces developed along the contact area of the inflatable can counteract the total external force originated by the flooding pressure. The feasibility of this resisting mechanism to contain flooding was demonstrated in the full-scale experimental evaluations (Barbero et al., 2013b, Sosa et al., 2014a). It is also at this stage when the interaction between the pressurized inflatable and the main tunnel liner is of particular importance. If the pressurization is achieved with compressed air, the pressure distribution can be considered uniformly distributed around the contact area. If the pressurization is done with water or other liquid, the pressure follows a hydrostatic distribution. Regardless of the fluid used for pressurization of the inflatable, the pressure is transferred, at the contact area, from the membrane throughout the lateral duct banks, invert, and ceiling of the tunnel, to the main liner of the tunnel. Depending on the characteristics of the tunnel, the following considerations will be necessary to assure the integrity of the liner during the pressurization of the inflatable plug:

– Verification of capacity of existing liner. Mid-size tunnels rail tunnels, with circular or near-to-circular cross sections of 5 to 7 meters in diameter, running under bodies of water such as channels, rivers, and bays, can have different types of liners depending on the type of ground in which they are surrounded by. In rail and metro tunnel systems sitting in soft grounds, it is common to find segmental liners that are built in one-pass system that provides stabilization and permanent service liner as the construction

advances. Materials typically used for this type of liner system include fabricated steel, cast iron, cast in place concrete, and precast concrete segmental liners (Bickel et al., 1996; Hemphill, 2013; Maidl et al., 2013). The contact between the outer surface of the segmental liners and the ground is achieved by grouting the surrounding annular void. The stability of the rings created by the segments derives from the contact and the support provided by the surrounding ground (AUA-ASCE, 2003). In wet grounds, segments are typically bolted to compress gaskets that prevent infiltration, and in dry grounds or some tunnels in rock, the liner segments can be left unbolted (ASCE, 1984; Bickel et al., 1996; BTS-ICE, 2004; Hemphill, 2013; Maidl et al., 2013). It might also be possible to find tunnels with reinforced or unreinforced monolithic concrete liners or dual liners that combine an outer segmental liner in contact with the ground with an inner cast-in-place concrete liner. These types of liners are typically designed to withstand the ground pressure, external water pressure, dead loads, surcharges and subgrade reactions and possibly internal pressure as a special loading case (Bickel et al., 1996; ITA, 2000; Maidl et al., 2013). In any of the liners listed above, an internal pressure will produce an expansion of the liner against the surrounding ground until the internal forces are balanced by the external loads and the tensile stresses in the tunnel liner. Depending on the magnitude of the internal pressure, the expansion will cause, for example, a concrete liner to crack, or will create stresses in segmental metallic liners that the connecting points may not able to resist (ASCE, 1984). In any case, an initial verification of capacity will be necessary to check that the existing liner (either bolted systems or steel reinforced concrete systems) can withstand an internal pressure equivalent to the maximum inflation pressure exerted by the inflatable plug.

- If the existing liner of the tunnel segment selected for installation of the inflatable plug cannot withstand the inflation pressurization, a retrofitting of that particular segment will be necessary.

26

Depending on the magnitude of the internal pressure expected during the pressurization of the inflatable, and the characteristics of the tunnel under consideration, some alternatives for reinforcing the existing liner include:

a) Application of sprayed concrete or shotcrete over additional reinforcement provided by steel wire mesh. The thickness and density of the steel wire mesh will depend on the magnitude of the pressure and on how much load is allowed to be transferred to the existing liner. In this alternative, a waterproof membrane can be installed between the existing liner and the new one. Additional reinforcement of this type of liner can also be provided by steel or macro-synthetic fibers embedded in the sprayed concrete matrix that in combination with conventional steel bars provide some additional crack resistance (Franzén, 1992; Zeidler and Jager, 2007). The surface finish of the sprayed concrete also needs to provide the texture needed to develop the frictional forces to contain the thrust originated by flooding pressure acting on the pressurized plug.

b) If the dimensions and the characteristics of the tunnel allow it, the installation of an additional precast concrete segmental liner that can be post-tensioned in situ with cable tendons can provide the compressive force necessary to counteract the tensile forces originated by the pressurization (Kenyon, 2015). The level of post-tensioning and thickness of the additional segments will depend on how much load is allowed to transfer to the existing liner. Additional anchoring points may be needed as well to carry out the thrust originated by the flooding pressures. Additional crack resistance can be achieved by adding fiber reinforcement to the individual segments of the liner (ACI 544.7R, 2016; Bakhshi and Nasri, 2016). Here again, a surface finish on the exposed surface of the segments will be needed to create the texture needed to develop the frictional resistance.

c) If the two previous options are not viable, another option for consideration is the installation of a steel liner. Steel liners are commonly installed in water conveyance tunnels or pressure tunnels. Steel liners are designed to resist the internal pressure and external pressures, as well as to prevent migration of tunnel leakage (ASCE, 1984, 1989, 2012; Brekke and Ripley, 1987; Bickel et al., 1996). If the tensile load-carrying capacity of the existing liner is limited, the steel liner can take a greater share, if not all the load, originated by the plug pressurization, limiting the deformations of the existing liner system. The stiffness the steel liner is proportional to the thickness and the modulus of elasticity of the steel, so the stiffer the liner, the greater the load-carrying capacity (Bickel et al., 1996). If some load sharing is allowed, the interaction with the contiguous existing liner as well as the soil-structure interaction with surrounding ground should be considered (ASCE, 1989). The void created between the existing liner, and the steel liner can be filled with grout or contact grout to seal remaining annular space left at the end of the retrofitting (AUA-ASCE, 2003). If some external leakage is expected, buckling of the steel lining could occur if unbalanced external pressures are applied to the new steel liner, so this possibility should be contemplated in the design too (ASCE, 1989; ASCE, 2012; BTS-ICE 2004). Some other innovative solutions have been proposed and implemented in the recent years for pressure tunnels. Glass fiber reinforced polymers (GRP), pre-stressed concrete liners and thin-walled precast reinforced concrete have been implemented in different pressure tunnels in America and Europe (Gober and Nackler, 2011; Grunicke and Ristic, 2012; Gerstner et al., 2013). Moreover, as in the previous liner options, the surface of the steel liner in contact with the inflatable plug will require additional conditioning to generate the required frictional resistance. This frictional surface can be provided by grouting

applied over the steel surface or by applying specialized paints that can generate the needed

frictional surface.

The definition of specific properties and a detailed design of any of the possible liners outlined above

is beyond the scope of this work. In the design, in addition to the loads, aspects such as accessibility to

the tunnel, and time available for completing the overall retrofitting of the selected tunnel segment, will

influence the final selection and its implementation. Finally, the decision on the lining method will be a

balance between cost and technical factors and the risk involved.

Summary and Conclusions

This work presented results of experimental work performed for the evaluation of initial deployment

and inflation of a large-scale inflatable structure installed in a tunnel segment for containment of flooding.

Folding and packing procedures necessary to prepare and install a prototype of a full-scale inflatable in

the tunnel segment were described. Results of initial deployment and inflation tests were presented and

discussed. Methods for evaluation of conformity and degree of contact of the membrane with the tunnel

section were introduced and implemented as well.

Experimental results indicate that systematic implementation of preparation procedures consisting of

folding and packing into a portable storage container lead to reasonably repeatable results during low-

pressure inflation tests.

Inflation tests demonstrated that a successful distribution of the membrane material over the tunnel

perimeter is achieved by a combination of gradual unrolling, first by self-weight and with the help of the

air inflow, and then by controlled membrane release. Gradual unrolling contributes to the coverage of the

lower portion of the tunnel while controlled membrane release contributes to improving the membrane

coverage in the upper portion of the tunnel.

Evaluations of conformity by local inspection allowed the initial assessment of local contact at critical locations. These critical locations included corners, changes of angle and transitions around the perimeter of the tunnel. Evaluation of conformity based on information provided by contact sensors placed along the contact zone corresponding to the cylindrical portion of the inflatable provided a greater insight of the degree of conformity of the membrane to tunnel section. Contact maps indicate that when the membrane is conforming well to the tunnel perimeter, the global percentage of contact at critical locations is relatively high (>80%). On the contrary, the presence of localized membrane bridging can significantly reduce the degree of local conformity.

For the proposed folding and preparation procedures, as well as for membrane configuration, and the inflation conditions implemented during the experimental evaluations, five factors were identified to influence the degree of conformity and local contact. Among these factors, the folding method and the membrane distribution during the initial unfolding and inflation define how good the global and local conformity will be; the shape of transitions at corners and angles determines the presence or absence of bridging membrane material; the amount of extra membrane material in the hoop perimeter of the inflatable contributes to improving the local conformity if properly distributed; and finally, the texture of the membrane and local imperfections along the contact area contribute to reducing the contact between the inflatable plug and the tunnel section.

REFERENCES

ACI 544.7R. 2016. Emerging Technology Report on Design and Construction of Fiber-Reinforced Precast Concrete Tunnel Segments. American Concrete Institute (ACI), Farmington Hills, MI.

American Underground Construction Association, 2003. AUA Guidelines for Backfilling and Contact Grouting of Tunnels and Shafts, Ed. R. W. Henn, ASCE Press & Thomas Telford, pp. 44-57.

ASCE, 1984. Guidelines for Tunnel Lining Design, Ed. T.D. O'Rourke, Reston, VA, pp. 11-23, 39-45.

ASCE, 1989. Tunnels and shafts. Civil Engineering Guidelines for Planning and Designing Hydroelectric Developments, Reston, VA, vol. 2, pp. 3-53 – 3-61.

ASCE, 2012. Steel Penstocks. ASCE Manuals and Reports on Engineering Practice No. 79, Ed. J. H. Bambei Jr., Reston, Virginia, pp. 59-72.

Bakhshi, M., Nasri V., 2016. STR-998: Design of Fiber-Reinforced Tunnel Segmental Lining According to New ACI Report. Proceedings of the Annual Conference of the Canadian Society for Civil Engineering: Resilient Infrastructure, London, Canada, June 1-4, 2016, pp. 1-10.

Barbero, E.J., Sosa, E.M., Martinez, X., Gutierrez, J.M., 2013 (a). Reliability Design Methodology for Confined High-Pressure Inflatable Structures. *Engineering Structures*, vol. 51, pp. 1-9.

Barbero, E.J., Sosa, E.M., Thompson, G.J., 2013 (b). Testing of Full-Scale Confined Inflatable for the Protection of Tunnels. Proceedings of the VI International Conference on Textile Composites and Inflatable Structures, K.-U. Bletzinger, B. Kröplin and E. Oñate, Editors. Structural Membranes 2013. Munich, Germany.

Barrie, A., 2008. Going Underground: Homeland Security Works on Tool to Prevent Tunnel Disasters. Published September 5, 2008, Last Accessed October 31, 2016. http://www.foxnews.com/story/0,2933,417461,00.html.

Beveridge, A., 1998. Forensic Investigation of Explosions. Page 41. Boca Raton. CRC Press.

Bickel, J.O., Kuesel, T.R, King, E.H., 1996. Tunnel Engineering Handbook. Kluwer Academic

    Publishers, Massachusetts, pp. 80-96, 298-310.

Brekke, T.L., Ripley, B.D., 1987. Design Guidelines for Pressure Tunnels and Shafts. Electric Power

    Research Institute, Final Report AP-5273 EPRI, pp. 5-17 – 5-32.

Brezhnev, V.A., Abramson, V.M., Zemelman, A.M., Vlasov, S.N., Koulaguin, N.I., Merkin, V.E.,

    Razbeguin, V.N., 2005. Russian underwater tunnels in the system of international transportation

    ways. *Tunnelling and Underground Space Technology*, vol. 20, pp. 595-599.

Carter, C., Byun, S., Marengo, B., 2001. Evaluation of Inflatable Dams for In-System Storage

    Utilization in CSO Abatement. Urban Drainage Modeling. Specialty Symposium on Urban Drainage

    Modeling at the World Water and Environmental Resources Congress 2001, R. W. Brashear and C.

    Maksimovic, Editors, Publisher: American Society of Civil Engineers, Orlando, Florida, United

    States, May 20-24, pp. 110-122.

Federal Highway Administration, 2003. Recommendations for Bridge and Tunnel Security. Blue Ribbon

    Panel Report, Report No. FHWA-IF-03-036, Washington, DC.

Fountain, H., 2012. Holding Back Floodwaters with a Balloon. The New York Times/Science

    Supplement, Published November 19, 2012, Last Accessed October 31, 2016,

    http://www.nytimes.com/2012/11/20/science/creating-a-balloonlike-plug-to-hold-back-

    floodwaters.html

Franzén, T., 1992. Shotcrete for Underground Support: A State-of-the-art Report with Focus on Steel-

    fibre Reinforcement. Tunnelling and Underground Space Technology, vol. 7, No. 4, pp. 383-391.

Fraser, T.M., 1989. The Worker at Work: A Textbook Concerned with Men and Women in the

Workplace, Page 323. CRC Press.

Gerstner, R., Netzer, E., Vigl, A., 2013. Long-term Behaviour of Pressure Tunnels. Geomechanics and Tunnelling, vol. 6, No. 5, pp. 407-421.

Ghavanloo, E., Daneshmand, F., 2010. Analytical Analysis of the Static Interaction of Fluid and Cylindrical Membrane Structures. *European Journal of Mechanics A/Solids*, vol. 29, pp. 600–610.

Gober, H., Nackler, K., 2011. First Operational Experience with a High-pressure Tunnel with Innovative Lining Methods. Geomechanics and Tunnelling, vol.4, No. 2, pp. 129 – 140.

Grunicke, U.H., Ristic, M., 2012. Pre-stressed Tunnel Lining – Pushing Traditional Concepts to new Frontiers. Geomechanics and Tunnelling, vol. 5, No. 5, pp. 503-515.

Haack, A., 2002. Current safety issues in traffic tunnels. *Tunnelling and Underground Space Technology*, vol. 17, pp. 117-127.

Hemphill, G.B., 2013. Practical Tunnel Construction. John Wiley & Sons, Inc., Hoboken, New Jersey, pp. 381-389.

Inouye, R., Jacobazzi, J., 1992. The Great Chicago Flood of 1992. *Civil Engineering-ASCE*, vol. 25(62), pp. 52–55.

ITA Working Group No. 2, 2000. Guidelines for the Design of Shield Tunnel Lining. Tunnelling Underground Space Technology, vol.15, pp. 303–331.

Katsumata, N., Natori, M.C., Yamakawa, H., 2014. Analysis of dynamic behavior of inflatable booms in zigzag and modified zigzag folding patterns. *Acta Astronautica*, vol. 93, pp. 45–54.

Kenyon, P., 2015. Breaking New Ground on LA Outfall Tunnel. TunnelTalk. Last accessed October 31, 2016, http://www.tunneltalk.com/Los-Angeles-USA-02June2015-Clearwater-Program-advances-design-of-critical-effluent-outfall-tunnel.php.

Kirkland, C.J., 2002. The fire in the Channel Tunnel. *Tunnelling and Underground Space Technology*, vol. 17, pp. 129-132.

Kuraray Co., 2013. Homeland Security: A Big Plug for Vectran, Published November 9, 2012, Last accessed October 31, 2016, http://www.kuraray.us.com/kuraray-vectran-material-used-in-subway-plug/.

Leitner, A., 2001. The fire catastrophe in the Tauern Tunnel: experience and conclusions for the Austrian guidelines. *Tunnelling and Underground Space Technology*, vol. 16, pp. 217-223.

Lindstrand Technologies, 2013. Inflatable Tunnel Plugs. Published December 17, 2013, Last accessed October 31, 2016, http://www.lindstrandtech.com/successful-inflatable-tunnel-plug-tests-netherlands/

Maidl, B., Thewes, M., Maidl, U., 2013. Handbook of Tunnel Engineering I: Structures and Methods. Wiley Ernst & Sohn, Berlin, Germany, pp. 45-59, 124-136.

Martinez, X., Davalos, J., Barbero, E., Sosa, E., Huebsch, W., Means, K., Banta, L., Thompson, G., 2012. Inflatable Plug for Threat Mitigation in Transportation Tunnels. *SAMPE 2012 Technical Conference Proceedings: Connecting the Advanced Materials Community*, Baltimore, MD, May 21-24, 2012. Society for the Advancement of Material and Process Engineering.

New York City [NYC] Office of the Mayor, 2013. PlaNYC: A Stronger, More Resilient New York. New York, NY. Published June 11, 2013, Last accessed October 31, 2016, http://www.nyc.gov/html/sirr/html/report/report.shtml.

Peil, K.L., Barbero, E.J., Sosa, E.M., 2012. Experimental Evaluation of Shear Strength of Woven Webbings. *SAMPE 2012 Technical Conference Proceedings: Connecting the Advanced Materials Community*, Baltimore, MD, May 21-24, 2012. Society for the Advancement of Material and Process

Engineering.

Post, Buckley, Schuh, and Jernigan, 2005. Hurricane Isabel Assessment, a Review of Hurricane

Evacuation Study Products and Other Aspects of the National Hurricane Mitigation and

Preparedness Program (NHMPP) in the Context of the Hurricane Isabel Response. National Oceanic

Atmospheric Administration (NOAA).

Rabkin, N., 2007. Passenger Rail Security, Federal Strategy and Enhanced Coordination Needed to

Prioritize and Guide Security Efforts. Publication GAO-07-583T, U.S. Government Accountability

Office.

Ricco, P., Baron, A., Molteni, P., 2007. Nature of Pressure Waves Induced by a High-speed Train

Travelling through a Tunnel. Journal of Wind Engineering and Industrial Aerodynamics, Vol. 95, pp.

781–808.

Richmond, D., Yelverton, J., Fletcher, E., Philips, Y., 1989. Physical correlates of eardrum rupture.

Annals of Otology, *Rhinology, and Laryngology*, vol. 109, pp. 35-41.

Rodler, J., Hagenah, B., 2012. Determination of Aerodynamic Burden in Rail Tunnels Using

Measurements and Simulation. Proceedings of the 6th International Conference on Tunnel Safety

and Ventilation, Graz, Austria, April 23-25, 2012, pp. 124-131.

Schenk, M., Viquerat, A.D., Seffen, K.A., Guest, S.D., 2014. Review of Inflatable Booms for

Deployable Space Structures: Packing and Rigidization. *Journal of Spacecraft and Rockets,* vol.

51(3), pp. 762–778.

Sklerov, F., Padilla, M., 2012. DEP Installs Two Inflatable Dams in Brooklyn to Help Improve New

York Harbor Water Quality. Published January 17, 2012, Last accessed October 31, 2016,

http://www.nyc.gov/html/dep/html/press_releases/12-02pr.shtml.

Sosa, E.M., Thompson, G.J., Barbero, E.J., 2014 (a). Testing of Full-Scale Inflatable Plug for Flood Mitigation in Tunnels. *Transportation Research Record: Journal of the Transportation Research Board*, vol. 2407(2), pp. 59-67.

Sosa, E.M., Thompson G.J., Barbero, E.J., Ghosh, S., Peil, K. L., 2014 (b). Friction Characteristics of Confined Inflatable Structures. *Friction*, vol. 2(4), pp. 365–390.

Sosa, E.M., Barbero, E.J., Thompson, G.J. 2014 (c). Design and Testing of Inflatable Plugs for Flood Containment in Tunnels. *Rev. Int. de Desastres Naturales, Accidentes e Infraestructura Civil*, vol. 14(1-2), pp. 39–58.

Sosa, E.M., Wong, C.S., Adumitroaie, A., Barbero, E.J., Thompson, G.J., 2016. Finite Element Simulation of Deployment of Large-Scale Confined Inflatable Structures. *Thin-Walled Structures*, vol. 104, pp. 152–167.

Stewart, C., 2006 (a). Blast Injuries, Page 33, Colorado Springs: Charles Stewart & Associates.

Stewart, C., 2006 (b). Blast Injuries: Preparing for the Inevitable. *Emergency Medical Practice*, vol. 8(4), pp. 1-28.

Stocking, A., 2013. An Inflatable Tunnel Seal Stops Flooding of World's Largest Undeveloped Uranium Mine. Last accessed October 31, 2016, http://www.petersenproducts.com/case_study/Large_Mine_Flooding_Remediation.aspx.

Tan, G.L., 2002. Firefighting in tunnels. *Tunnelling and Underground Space Technology*, vol. 17, pp. 179-180.

TCRP Report 86/NCHRP Report 525, 2006. Public Transportation Security. Volume 12. Making Transportation Tunnels Safe and Secure. Transportation Research Board of the National Academies, Washington, D.C.

The British Tunnelling Society (BTS), the Institution of Civil Engineers (ICE) and Crown, 2004, Tunnel

Lining Design Guide. Thomas Telford, London, pp. 59-95.

Zeidler, K., Jager, J., 2007. Fiber Reinforced Shotcrete for Tunnel Linings. Proceedings of the First

International Conference on Advances in Concrete Technology (RAC07), Fiber Reinforced Shotcrete

for Tunnel Linings, September 19-20, Washington, D.C.

Zimmerman, R., 2014. Planning Restoration of Vital Infrastructure Services Following Hurricane Sandy:

Lessons Learned for Energy and Transportation. *Journal of Extreme Events*, vol. 1(1)-145004, pp.1-

38.

FIGURES AND TABLES

(a)   (b)
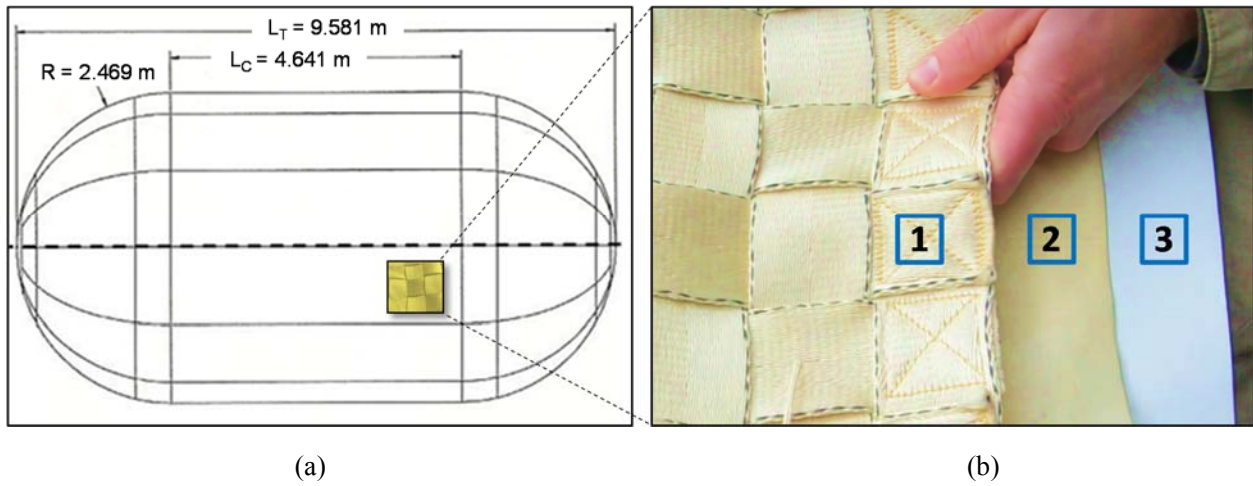
Fig. 1. Inflatable Plug: (a) Dimensions for unconstrained inflation; (b) Membrane architecture: [1] External macro fabric comprised of woven webbings; [2] Intermediate protective fabric; [3] Internal bladder.
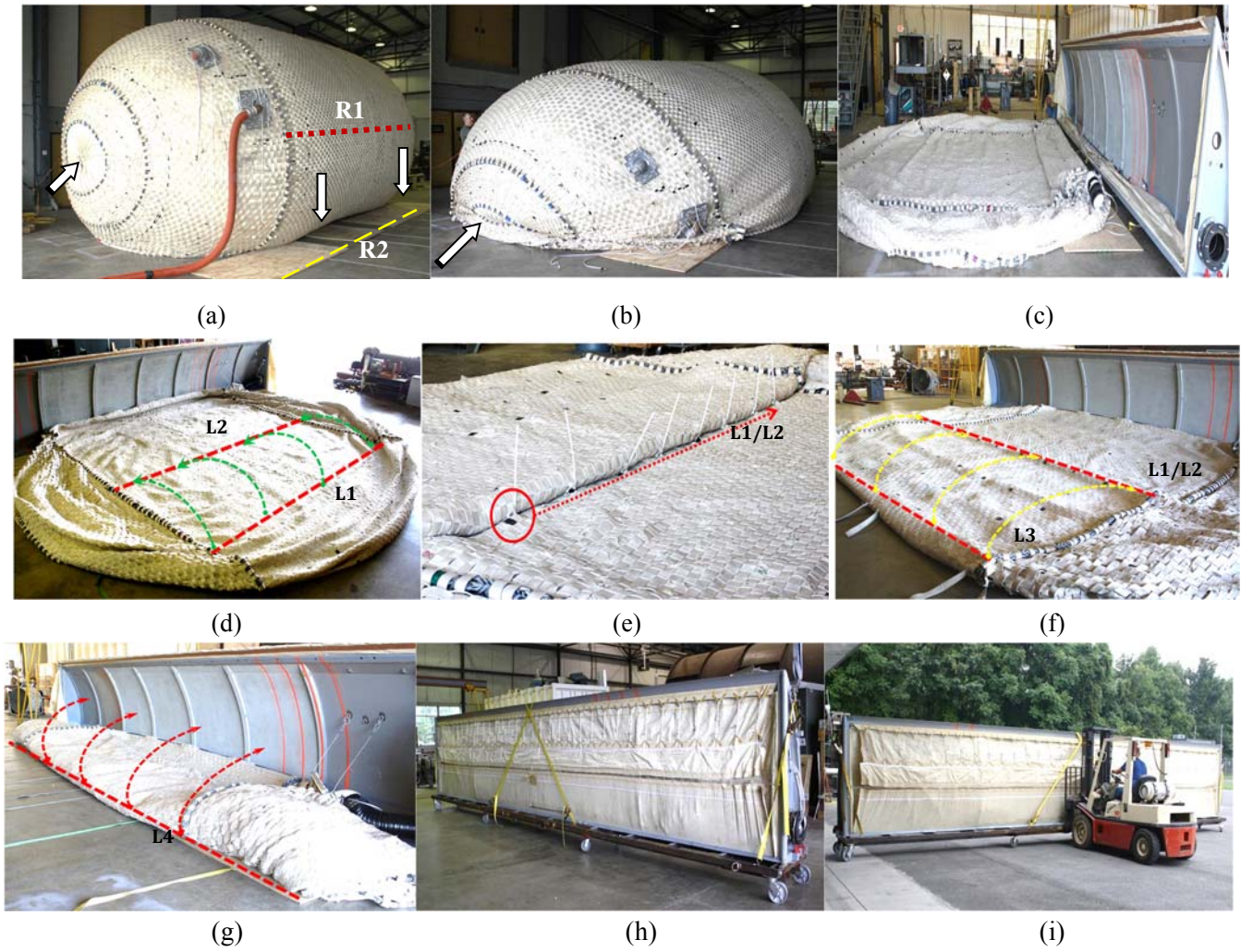
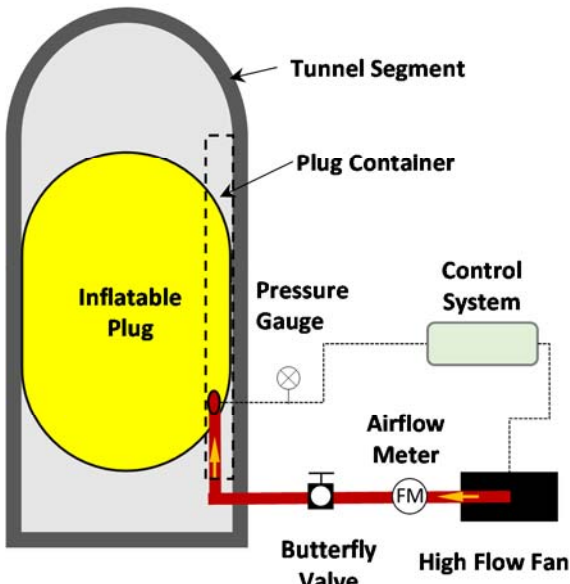**Fig. 2.** Inflatable Plug: Folding and packing sequence.
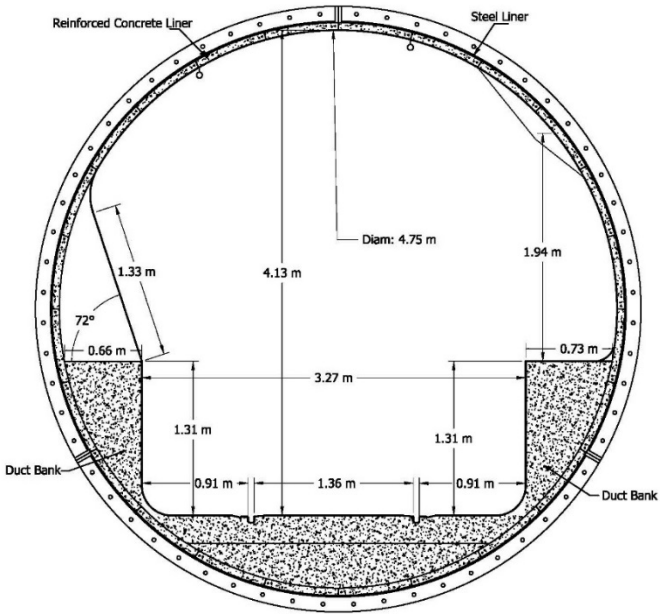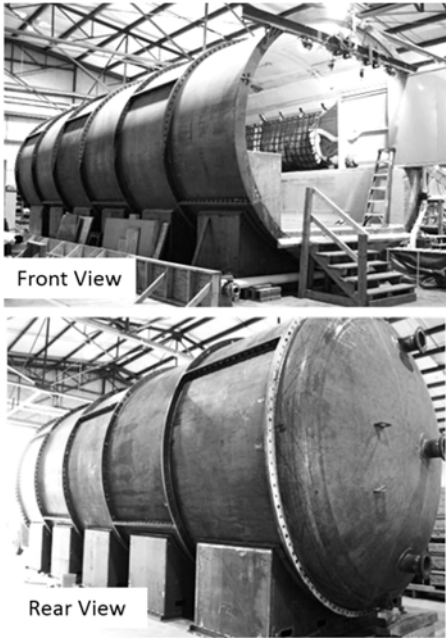
<table>
<tr><td>(a)</td><td>(b)</td></tr>
</table>

Fig. 3. Full-scale tunnel mockup: (a) Cross-section and dimensions; (b) Segment used for testing purposes.
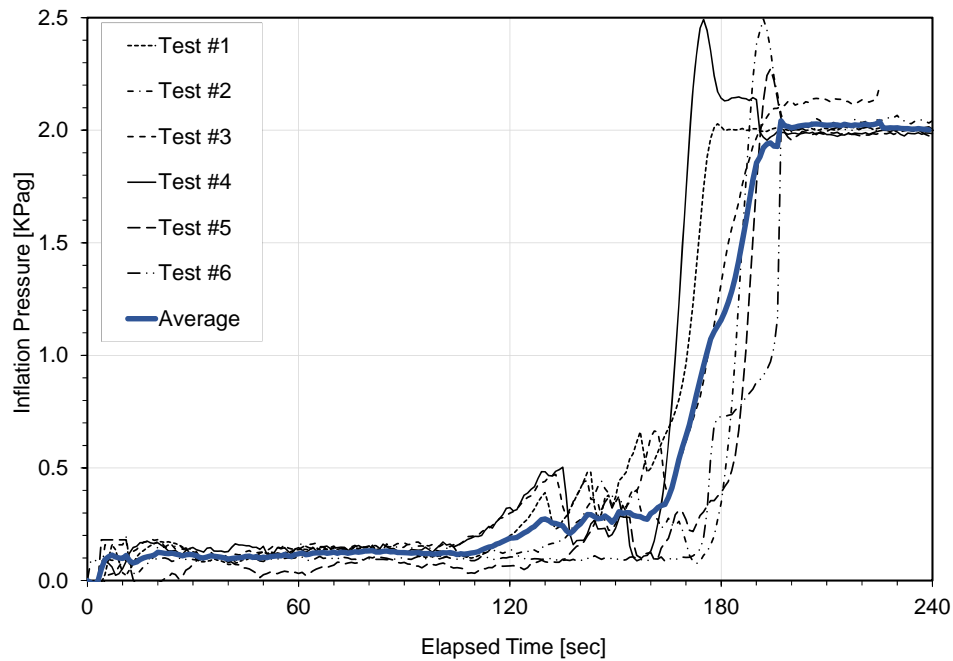
(a)

(b)
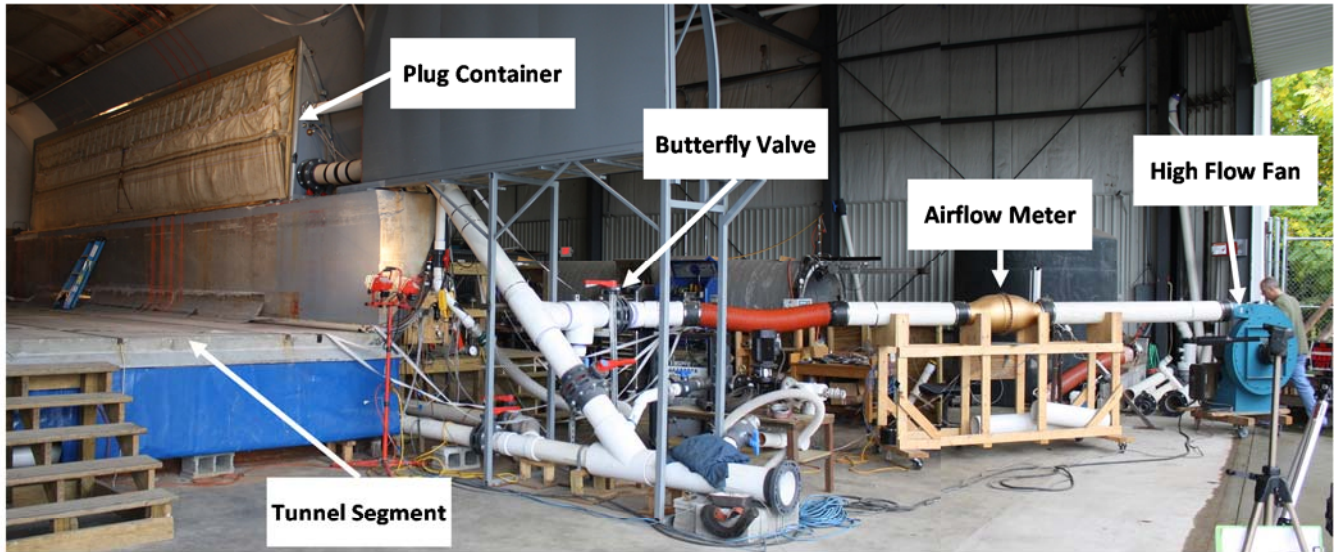
(c)

Fig. 4. (a) Components of inflation system; (b) Schematic overhead view of full-scale test setup; (c) Tunnel section prepared for a deployment and inflation test.
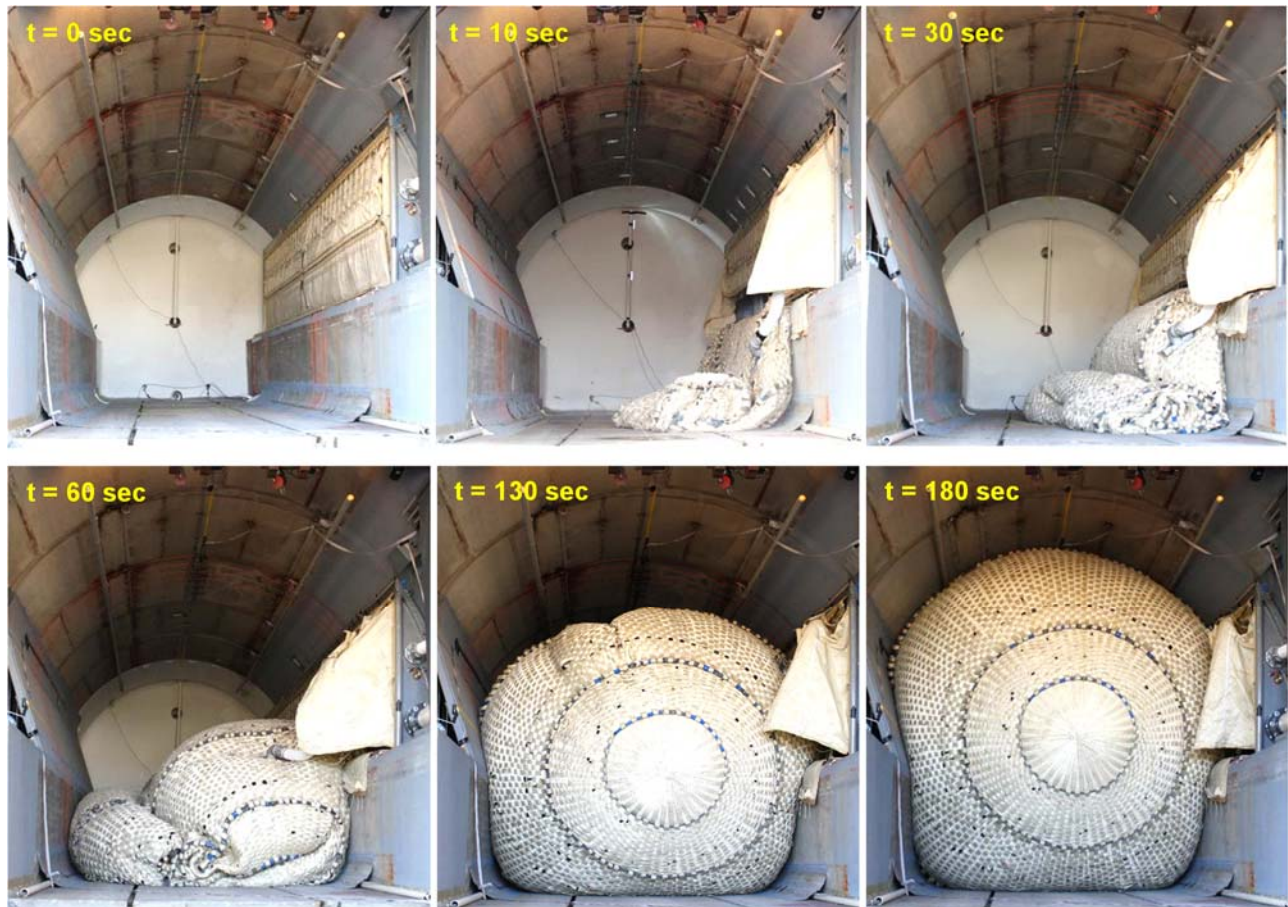
Fig. 5. Initial deployment and inflation sequence corresponding to Test #4.
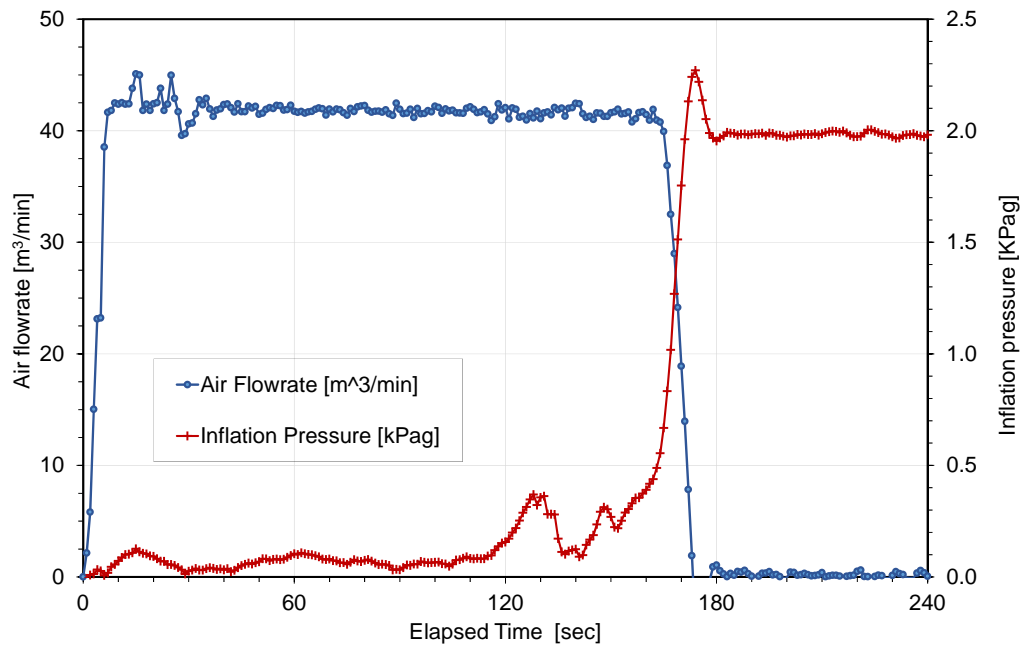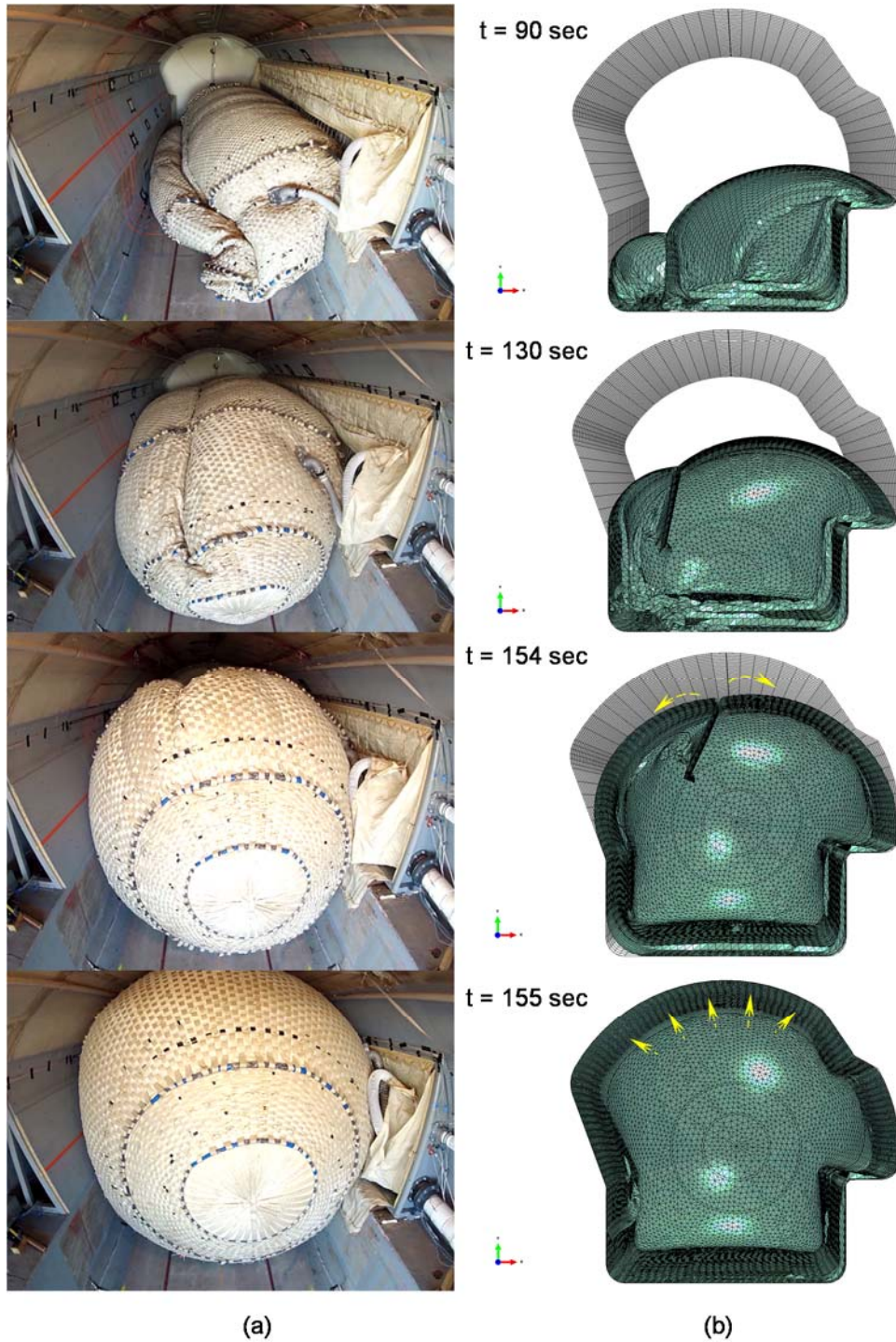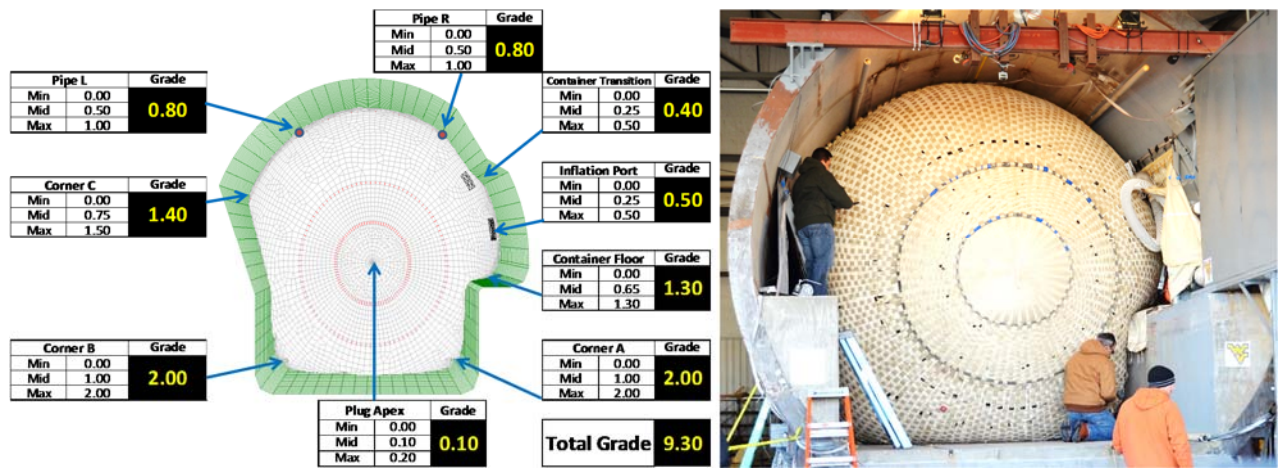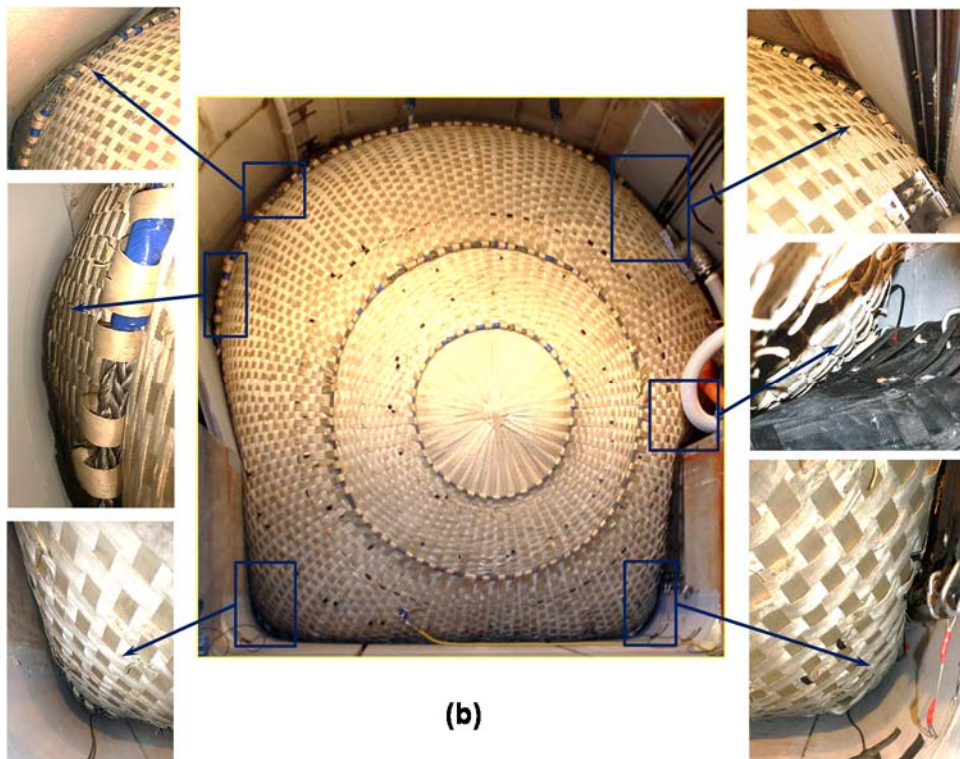
(a)

(b)

Fig. 6. (a) Air flow rate and inflation pressure for Test #5; (b) Inflation pressures for Tests #1 to #6.

t = 90 sec

t = 130 sec

t = 154 sec

t = 155 sec

(a)   (b)

Fig. 7. Sequence of membrane release: (a) Top view of Test #5; (b) Finite Element Simulation, transversal cuts show the plug interior and arrows indicate the direction of membrane movement once it has been released (Sosa et al., 2016).
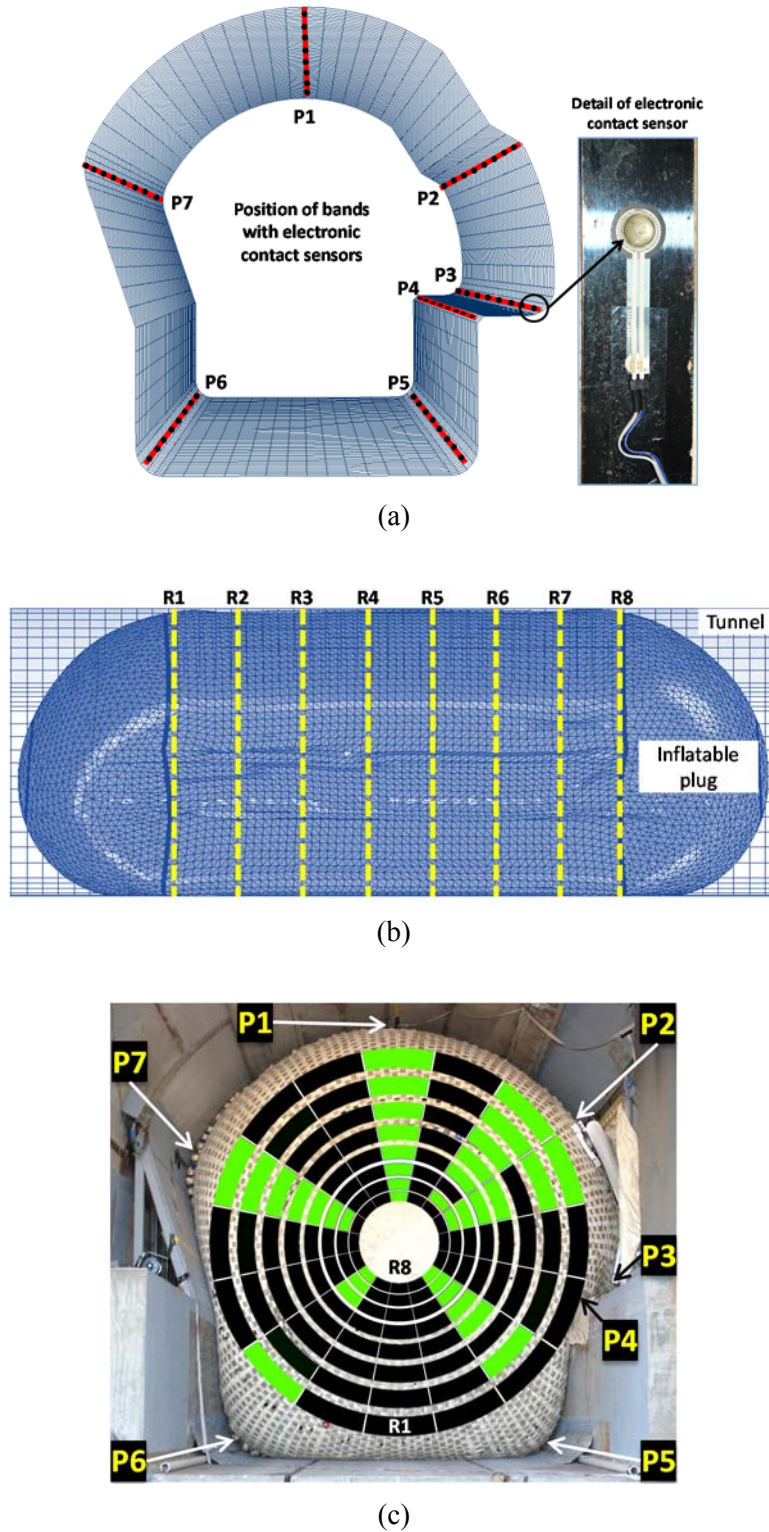
(a)

Fig. 8. (a) Assessment form and implementation of evaluation method M1; (b) Close-up views of critical locations captured during the implementation of evaluation method M1.

(a)

(b)

(c)

Fig. 9. (a) Position of bands with contact sensors for evaluation method M2; (b) Longitudinal distribution of contact sensors, where Ri correspond to one ring of the contact map; (c) Contact map (black stripes indicate no contact or no sensor at that position, and green stripes indicate membrane material touching contact sensor).
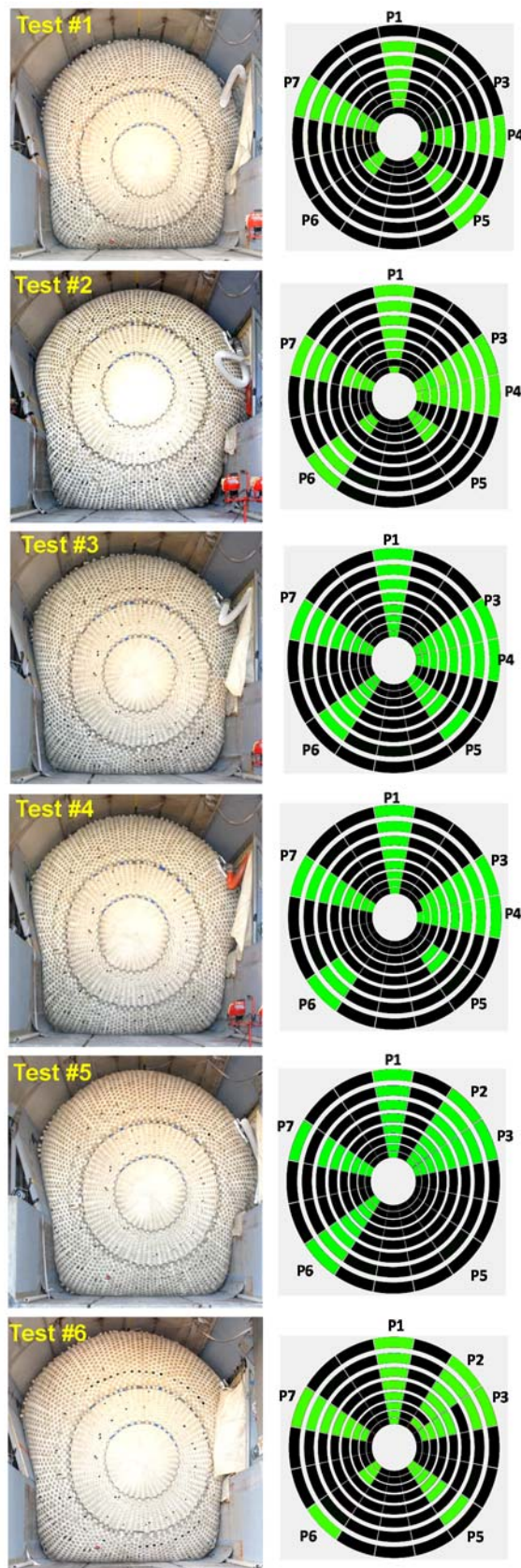
Fig. 10. Contact maps at an inflation pressure of 2 kPag.

Table 1. Inflation times and scores obtained from evaluation methods M1 and M2.

Test #	Inflation Time [Minutes]	Method M1 [Scale: 0-10]	Method M2 [Scale: 0-100%]
1	2.84	7.6	60%
2	3.10	8.2	81%
3	2.90	9.1	94%
4	2.76	8.9	75%
5	2.82	7.5	81%
6	3.12	9.3	77%
Average	**2.92**	**8.4**	**78%**
Std. Dev.	0.15	0.77	11%
C.o.V.	5.2%	9.2%	14.1%

Table 2. Estimation of force on a tie-down during initial inflation at the onset of breakage.

R	P_i	Hoop stress	L	Total hoop force	Number of tie-downs	Force per tie-down
[m]	[kPag]	[kN/m]	[m]	[kN]	[ ]	[kN]
~2.3	~0.70	1.61	4.641	7.47	10	0.75

Table 3. Summary of position and number of sensors detecting contact for method M2.

Test #	P1	P2	P3	P4	P5	P6	P7	Total	M2 %
1	6	n/a	0	6	6	3	8	29/48	60%
2	7	n/a	8	8	4	5	7	39/48	81%
3	8	n/a	8	8	6	7	8	45/48	94%
4	8	n/a	7	8	2	3	8	36/48	75%
5	8	8	8	n/a	0	8	7	39/48	81%
6	8	6	6	n/a	6	4	7	37/48	77%
Avg. # of sensors detecting contact	7.5	7.0	6.2	7.5	4.0	5.0	7.5	38	78%
No. of available sensors	8	8	8	8	8	8	8	48	
Local % of contact	94%	88%	77%	94%	50%	63%	94%	78%	